Maintaining cell depth viability: on the efficacy of a trimodal scaffold pore architecture and dynamic rotational culturing

Conor Timothy Buckley · Kevin Unai O'Kelly

Abstract Tissue-engineering scaffold-based strategies have suffered from limited cell depth viability when cultured in vitro with viable cells typically existing at the fluid-scaffold interface. This is primarily believed to be due to the lack of nutrient delivery into and waste removal from the inner regions of the scaffold construct. This work focused on the assessment of a hydroxyapatite multi-domain porous scaffold architecture (i.e. a scaffold providing a discrete domain for cell occupancy and a separate domain for nutrient delivery). It has been demonstrated that incorporating unidirectional channels into a porous scaffold material significantly enhanced initial cell seeding distribution, while maintaining relatively high seeding efficiencies. In vitro static culturing showed that providing a discrete domain for nutrient diffusion and metabolic waste removal is insufficient to enhance or maintain homogeneous cell viability throughout the entire scaffold depth during a 7-day culture period. In contrast, scaffolds subjected to dynamic rotational culturing maintained uniform cell viability throughout the scaffold depth with increasing culturing time and enhanced the extent of cell proliferation (∼2–2.4-fold increase) compared to static culturing.

1 Introduction

Scaffold-based bone tissue engineering has made significant advances in creating scaffolds with well defined architectures with the advent of solid free-form (SFF)

fabrication [1–4] and optimization of alternative techniques such as freeze-drying [5–7], foam reticulate method [8], porous slip casting [9, 10], among others.

Despite advances in fabrication methods and biomaterial interactions significant questions with respect to optimization for tissue regeneration remain. In vitro studies have repeatedly demonstrated predominant recurring issues with scaffold-based approaches when attempting to maintain cell depth viability and tissue formation. This may be explained by the lack of nutrient delivery to and waste removal from the inner regions of a scaffold [11, 12]. In addition, if the pore size or interconnectivity is too small, cells can occlude them, preventing further cell penetration and widespread bone formation [13].

Many of the existing scaffold architectures provide a single domain into which cells are seeded and, during in vitro culturing, proliferate and migrate to a small extent into the available pores [4]. In these scaffolds, a single pore system must accommodate the conflicting effects of cell proliferation and matrix formation with the need for greater nutrient delivery and metabolic waste removal (i.e. with increased cell proliferation, the availability of nutrients becomes diminished). This inevitably leads to a thin layer of tissue formation at the periphery of the scaffold [14], and a necrotic region at the core of the scaffold. Exclusive peripheral tissue formation may be a manifestation of the fact that as cells within the pores of the scaffold begin to proliferate and secrete extracellular matrix (ECM), they simultaneously begin to occlude the pores and decrease the supply of nutrients to the interior [15]. Scaffolds with limited interconnectivity/fenestration may also accelerate this phenomenon. The key parameter responsible for this phenomenon is believed to be the limited transport of oxygen to the interior regions of a scaffold construct [12, 16–21]. Significant work has also been undertaken

C. T. Buckley (✉) · K. U. O'Kelly
Trinity Centre for Bioengineering, School of Engineering,
Trinity College Dublin, Dublin, Ireland
e-mail: conor.buckley@tcd.ie

using bioreactor based systems in which scaffolds are cultured under dynamic conditions to overcome oxygen diffusion and nutrient limitations. These applied dynamic culturing conditions have been shown to enhance developing neo-tissue formation through enhanced nutrient delivery and metabolic waste removal [22–24].

In addition, scaffold architectures have been developed with distinct and separate domains [10, 25–27] in order to minimize diffusional constraints. In this configuration a porous scaffold can possess meso-pores ($\sim$90–200 μm) in which cells proliferate and lay down new matrix and also larger scale channels (300–500 μm) which provide for higher levels of nutrient and oxygen delivery and metabolic waste removal through diffusion. For example, it has been demonstrated that cell coverage increased with increasing channel diameter within porous hydroxyapatite (HA) scaffolds with a centrally aligned channel [10].

In our laboratory, we have recently developed a hydroxyapatite multi-domain porous scaffold architecture (i.e. a scaffold providing a discrete domain for cell occupancy and a separate domain for nutrient delivery) [28]. The objectives of creating a multi-domain scaffold are to enhance for cell-seeding/distribution and proliferation during short term in vitro culture prior to implantation. The work presented herein, assesses such architectures in terms of cell seeding and the resulting cell-depth viability during 7 days of culturing under both normal static diffusion-based and dynamic rotational regimes.

2 Materials and methods

2.1 Scaffold fabrication

Porous hydroxyapatite (HA) scaffolds were fabricated as previously described [28], Briefly, an aqueous suspension consisting of 36% w/v HA powder (Plasma Biotal., Tideswell, Derbyshire, UK), 2 wt% Darvan® 811 dispersant (R.T. Vanderbilt Company, Inc., USA) and a binding agent, liquid methylcellulose (Methocel® 60HG, Fluka, 2.5% (w/v), Sigma-Aldrich, Ireland) was prepared, homogenised for 12 h and degassed under vacuum for 1 h prior to use. The suspension was cast into stainless steel rings, placed on the cooling shelf of a freeze-dryer (Advantage EL, VirTis Co., Gardiner, NY) and cooled at a constant cooling rate to a desired final freezing temperature ($T_f = -40°C$) and finally sublimated under vacuum (200 mTorr) for 17 h at a temperature of 0°C [5, 7]. Green body cakes obtained from the freeze-drying process were impregnated with a low melting temperature (44–46°C) paraffin wax to facilitate the introduction of unidirectional channels in the longitudinal direction. Channels with diameters of 500 μm and 1 mm spacing (centre–centre) were introduced through CNC machining. Scaffold cylinders (5 × 4 mm) were cored and sintered to a final temperature of 1350°C. An overview of the fabrication process is presented in Fig. 1a and b. The terminology used to describe the various architectures in

Fig. 1 a Process overview for fabrication of scaffolds, **b** Experimental CNC set-up for the introduction of unidirectional channels. [1]Mandrel and drill [2]Wax infiltrated HA freeze-dried cake and [3]Air jet. **c** Rotational bioreactor system
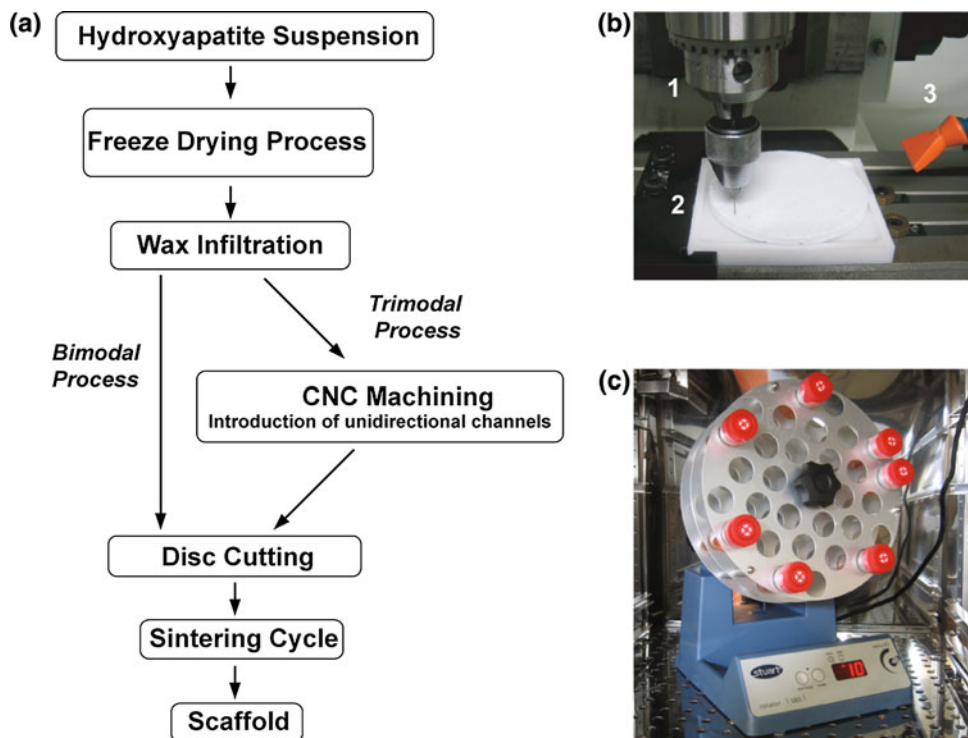
Table 1 Scaffold terms used to define various scaffold architecture types

Scaffold term	Scaffold type
Bimodal	Scaffold produced through the freeze drying process containing both micro- and mesopores
Trimodal	CNC machined freeze dried bimodal scaffold containing micro-, mesopores and unidirectional channels

this work is presented in Table 1 with representative images of trimodal scaffolds presented in Fig. 2.

2.2 Assessment of seeding efficiency, cell proliferation and viability

In all experiments, MC3T3-E1 mouse clonal osteogenic cells (sub-clone 4) were maintained in α modified Eagle's medium (α-MEM) supplemented with L-glutamine (2 mM), sodium pyruvate (1 mM), penicillin (100 U/ml), streptomycin (100 µg/ml) and 10% fetal bovine serum (FBS). Seeding efficiency, and cell proliferation for 7-day culture experiments was quantified through measurement of the DNA content using the Hoechst 33258 dye assay as described previously [29].

Spatial distribution of cells throughout scaffold constructs was determined using an MTT [3-(4,5-dimethyl-thiazol-2-yl)-2,5-diphenyl tetrazolium bromide] assay. Scaffold samples were first cut in half, washed in PBS and incubated with 2 ml of the MTT (2 mg/ml in PBS) stock solution at 37°C for 1 h. Viability and distribution were evaluated qualitatively by a dark blue stain, indicating that reduction of MTT to formazan had occurred. For cellular viability and distribution images 3 h post seeding, a further incubation period with the MTT assay of 1 h is added to the time frame of assessment.

2.3 2D and 3D time-dependent cell seeding

To ascertain the time required for cell attachment on 2D surfaces, a time dependent analysis was carried out on 2D non-porous HA ceramic substrates, fabricated in a similar fashion to 3D scaffolds without the freeze drying procedure. Initial seeding density was adjusted to 2.5×10^4 cells/cm^2. Time intervals post seeding of 5, 30, 45, 60, 90, 120 and 180 min were examined.

An investigation was also carried out to assess if a time-dependent relationship existed for the mesoporous domain of 3D constructs. For this purpose, bimodal scaffolds were seeded (3×10^5 cells/scaffold) and assessed at specific time points (30, 60, 120 and 180 min) after washing with PBS (×3).

2.4 Trimodal scaffold seeding volume dependency

One of the initial roles of this study was to optimize the seeding efficiency of trimodal scaffolds. Therefore, a study was performed to assess if the cell seeding efficiency of trimodal scaffolds was dependent on the total volume of cell suspension delivered. Trimodal scaffold constructs were seeded with 3×10^5 cells while varying the volume of suspension (25, 50 and 100 µl) and assessed after 180 min.

2.5 Static and dynamic rotational culturing of scaffolds

Bimodal and trimodal porous scaffolds were statically seeded with 3×10^5 cells and incubated for 3 h prior to static- or dynamic rotational-culturing for a period of 7 days. For the dynamic rotational culturing regime, constructs were placed into the bottom of 30 ml polypropylene tubes with supplemented medium. The 30 ml tubes were capped and inserted into a rotator wheel (Stuart® Rotator SB3, Lennox Laboratory Supplies Ltd., Ireland) inclined at an angle of approximately 15° in an incubator maintained
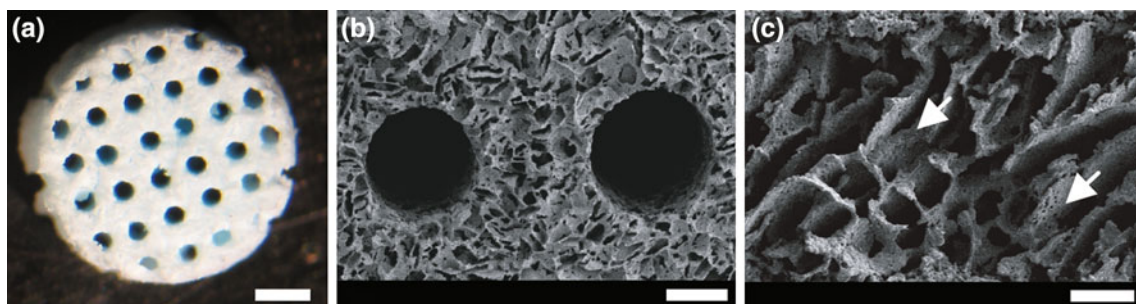
Fig. 2 a Light micrograph of the scaffold architecture of trimodal scaffolds produced through the freeze drying process, scale bar: 1 mm. **b** SEM image of a unidirectional channels (Ø 500 µm) surrounded by the mesoporous region, scale bar: 250 µm. **c** Higher magnification SEM image showing meso- and micropores (highlighted by white arrowheads), scale bar: 100 µm

at 37°C (Fig. 1c). Each tube contained only one scaffold and rotation was performed clockwise around the central axis of the rotator wheel with a rotation radius of 10 cm with a rotation speed of 10 r.p.m. Scaffold groups (i.e. bimodal static, trimodal static, bimodal rotational and trimodal rotational) were assessed after 1, 3, 5 and 7 days of culture to examine for cell proliferation and viable distribution.

2.6 Statistical analysis

Numerical and graphical results are reported in the form of mean ± standard deviation (SD). All statistical analyses were performed using GraphPad Prism software (Version 4.3) using either one way ANOVA with Tukey's post-hoc test for multiple comparisons, or two-way ANOVA with Bonferroni post-tests.

3 Results

MC3T3-E1 cells attached to non-porous HA substrates in an increasing time-dependent manner (Fig. 3a), from a minimum of 46.6% (± 5.8, $n = 5$) after 5 min increasing to a maximum of 75.7% (± 6.0, $n = 5$) after 60 min, with a plateau existing after this time point. There was a statistically significant difference between the percentage cell attachment measured after 5 min compared to all subsequent time points ($P < 0.05$). No difference was found between 60, 90, 120 and 180 min post seeding groups ($P > 0.05$).

A similar study was carried out for bimodal porous scaffolds to investigate if this time-dependent relationship also existed for 3D constructs. It was found that the number of cells within bimodal scaffolds did not change with time ($\sim 80\%$) with no statistical difference ($P > 0.05$) found for any of the time points investigated (Table 2).

For increasing seeding suspension volume there was an inverse relationship in the seeding efficiency obtained, from a maximum of 85.4% (± 4.9, $n = 4$) for 25 µl, decreasing to 67.7% (± 2.2, $n = 4$) for 50 µl with a minimum of 43.8% (± 3.2, $n = 4$) for 100 µl (Fig. 3b). Although a lower seeding volume (25 µl) produced higher seeding efficiencies, MTT staining demonstrated that low seeding volumes (i.e. 25 µl) resulted in poor penetration and distribution of cells into the scaffold volume and were ultimately confined to the top surface.

Initial homogenous seeding distribution was observed for trimodal scaffolds with uniform staining throughout the entire scaffold depth (Fig. 4). In contrast, seeded bimodal scaffolds did not demonstrate this homogeneous staining indicating limited penetration of cells through the porous scaffold material. Comparing the top surfaces of both bimodal and trimodal scaffolds, for bimodal scaffolds a darker blue stain is present which indicates a greater density of cells present. This intensity of stain was not observed for trimodal scaffolds, with both cross-sectional and top surfaces of trimodal scaffolds exhibiting similar stain intensity, demonstrating a more homogeneous distribution.

After 7 days, both bimodal and trimodal static culturing groups exhibited intense staining for viable cells in the outer periphery of the scaffold volume, indicating significant cellular proliferation had occurred in the outer regions. Compared to the staining intensity observed post-seeding of trimodal scaffolds, no significant increase in staining had developed within the inner core region by day 7 demonstrating limited or insignificant cell proliferation had occurred within this region. For the dynamic rotational groups, bimodal scaffolds demonstrated penetration of
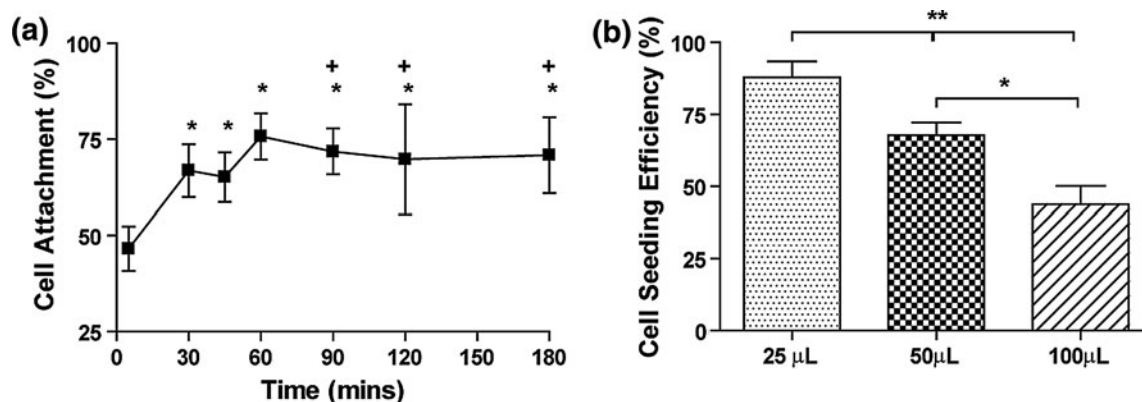
Fig. 3 **a** Time course evaluation of cell attachment to 2D non-porous HA substrates. * Significance compared to 5 min ($P < 0.05$, $n = 5$), [+] No significance compared to 60 min ($P < 0.05$). **b** Seeding efficiency (%) of cells within trimodal scaffolds 3 h post-seeding.

All scaffolds were seeded with 3×10^5 cells while varying the volume of suspension delivered (25, 50 and 100 µl, $n = 4$ for each group). Significance: (* $P < 0.05$ and ** $P < 0.01$)

Table 2 Seeding efficiency (%) of cells of bimodal scaffolds at various time points (30, 60, 120 and 180 min) post-seeding

Time (min)	Seeding efficiency (%)	SD (%)	n
30	78.7	5.6	5
60	82.2	5.1	5
120	81.5	13.6	5
180	79.1	4.7	5

SD standard deviation, n number of samples. No significance was found between any of the time points investigated ($P > 0.05$)

viable cells towards the core region compared to the corresponding static group, although no staining was observed within the core region. However, for trimodal groups, a homogeneous staining for viable cells was present throughout the scaffold depth.

Under static culturing conditions, both bimodal and trimodal scaffolds demonstrated an increase in cell number with increasing time in culture (Fig. 5). After 1 day of culturing, no statistical difference in cell number existed between bimodal and trimodal scaffold groups for either static or dynamic culturing regimes. However for each of the subsequent time points, higher cell numbers were observed for bimodal scaffolds compared to trimodal scaffolds subjected to static culturing ($P < 0.05$). For

dynamic rotational cultures, no difference in cell number was observed between bimodal and trimodal scaffolds at any of the time points investigated ($P > 0.05$). Comparing culturing regimes, for bimodal groups, after 7 days there was a 2-fold increase in the number of cells within dynamically cultured scaffolds compared to static conditions. Likewise, dynamically cultured trimodal scaffolds exhibited a 2.4-fold increase in cell number compared to statically cultured trimodal scaffolds after 7 days.

4 Discussion

The static seeding method is often associated with low seeding efficiencies and non-uniform cell distributions within scaffolds, which is partially due to the manual- and operator-dependent nature of the process [30]. In this study, 2D cell attachment was observed to occur in a time-dependent fashion reaching a plateau after 60 min. Similar observations have been made for seeding anorganic bovine matrix with primary culture neonatal rat osteoblastic cells with an increasing trend in cell attachment up to 90 min post-seeding [31]. This time-dependent trend could not be replicated in 3D bimodal scaffold studies, with the seeding efficiency of constructs remaining constant at ∼80%. This
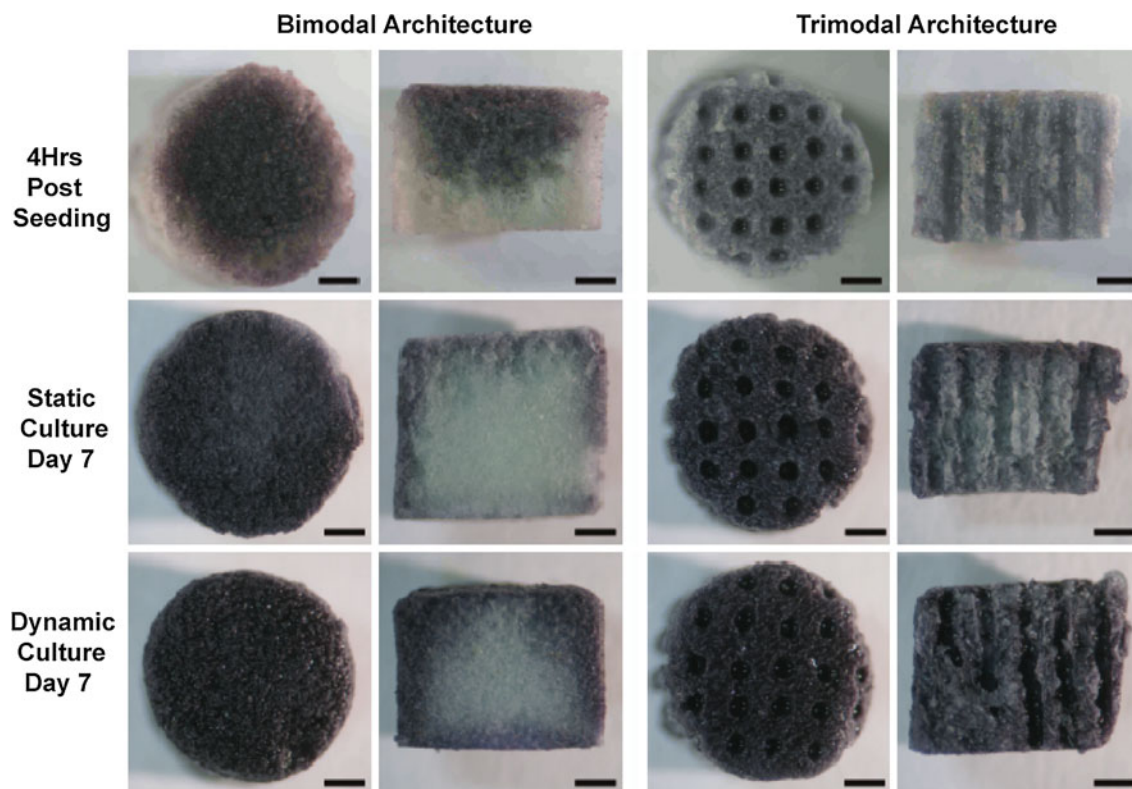
Fig. 4 Comparative MTT staining of surface and longitudinal cross sections of bimodal and trimodal scaffolds 7 days post seeding. Scaffolds were subjected to either static or dynamic culturing. Scale bar is 1 mm
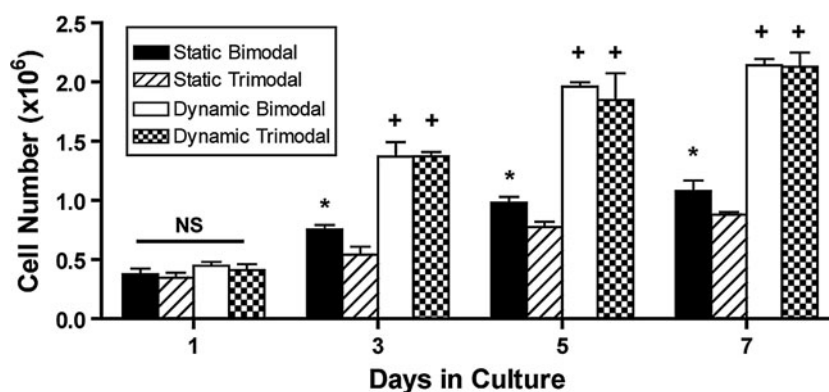
Fig. 5 Comparative growth kinetics over a 7-day period of MC3T3-E1 cells cultured on bimodal and trimodal HA scaffolds subjected to either static or dynamic culture conditions. The data represents the mean of triplicate samples ± the standard deviation. NS: no significance, * $P < 0.05$ compared to static trimodal scaffolds at same time point, $^+$ $P < 0.001$, compared to same architecture scaffold type subjected to static culture at the same time point

may not necessarily imply that cell adhesion has been attained after 30 min. It is more probable that cells occupying the pores could not be removed through washing. The lack of a time dependency trend for maximal cell seeding of 3D scaffolds compared to 2D surfaces indicates that there does not appear to be a minimum time required for enhanced seeding of porous scaffolds. This may prove useful from a clinical perspective in relation to immediate in vivo implantation post seeding, without any incubation period required.

For seeding of three-dimensional scaffolds it was hypothesised that the cell seeding inefficiencies commonly observed for static seeding, ranging from approximately 25% [32] to greater than 75% [12, 33], for different cell and scaffold types, may in part be related to the volume of cell suspension being delivered to the scaffold, with higher seeding volumes producing lower seeding efficiencies. Experiments showed a decreasing trend in the number of cells within scaffolds for increasing volume of cell suspension delivered from a maximum of 85.4% for a seeding volume of 25 µl decreasing to a minimum of 43.8% for 100 µl. Therefore, it is the saturation of the scaffold itself that inhibits further cell attachment and explains the observation of a decreasing efficiency trend, while increasing the volume of cell suspension.

The data obtained may in part also explain some of the large variations in cell seeding efficiency data observed in the literature [12, 32, 33]. Although lower seeding volumes were found to yield higher seeding efficiencies, limited cell penetration was found to exist thus producing poor cell distributions, with the majority of cells being confined to the top surface of the scaffolds. Therefore, high seeding efficiencies alone may not be the most appropriate metric for evaluation purposes and should perhaps be used in conjunction with initial viable cell distributions.

Initially, trimodal scaffolds exhibited superior homogeneous cell distribution throughout the entire scaffold depth compared to bimodal scaffolds. This enhancement is due to the presence of the channels within the mesoporous phase, allowing the cell suspension to be more easily absorbed into the mesoporous domain depth. This highlights one of the significant benefits of incorporating unidirectional macrochannels into porous scaffold architectures. In contrast, bimodal scaffolds exhibited limited cell penetration, with a greater density of cells being confined to the top surface and the outer peripheral regions (<1 mm) of the scaffolds. The overall qualitative results of cellular distribution within trimodal scaffolds using the static seeding method proved to be a highly effective and a simple method compared to the cellular distributions obtained for seeding of bimodal scaffolds under identical conditions. The relatively poor penetration of cells for bimodal scaffolds is comparable to previous observations made when statically seeding porous β-TCP ceramic scaffolds [34].

Dynamic culturing conditions were shown to enhance cellular proliferation (2–2.4-fold increase) and cell viability distribution compared to static culturing conditions. This increase is most likely due to enhanced nutrient supply and more efficient metabolic waste removal from the interior regions of scaffold constructs due to constant mixing of the medium caused by rotation of the constructs. Due to this, a more favourable environment was promoted in which cells could remain viable and therefore proliferate to a greater extent compared to static cultures. Interestingly, comparing trimodal and bimodal scaffolds at each specific time point there was no statistically significant difference in cell number within scaffolds which were dynamically cultured. Viability staining of these scaffold groups over time, demonstrated very different viable cell distributions. After 7 days static culturing, it was evident

that a non homogenous cell distribution was beginning to develop within trimodal type scaffold structures which had initially been shown to be homogeneously seeded.

In the case of bimodal scaffolds after 7 days of static culturing, only viable cells were observed to exist within the outer periphery (~ 500 μm), and cells had not migrated to any extent towards the inner core region. It is therefore feasible to hypothesise that under static culturing conditions, nutrient transport and waste-product efflux was insufficient to maintain or enhance cell viability in the interior regions of both these scaffold types. Although bimodal scaffolds initially exhibited poor viable cell distributions, it was observed that significant cell migration occurred when scaffolds were subjected to dynamic culture conditions. This highlights that the mesoporous architecture of these scaffolds produced through the freeze-drying technique was not inhibiting in terms of pore size and pore interconnectivity.

From an in vivo perspective, the observations from the static culturing experiments may give rise for significant concern when developing bone tissue engineering strategies, due to the non-homogeneous cell viability after 7 days. In the early stages of scaffold implantation, prior to vascularisation, a cell seeded scaffold relies solely on the diffusion of oxygen through the blood itself [35]. Therefore it is pertinent to maximize diffusional effectiveness of scaffolds and to subsequently enhance rapid vascularisation in order to encourage cell migration and maintain cell depth viability. By providing a direct conduit, the channels may facilitate or enhance vascularisation post-implantation and during the progressive fracture healing process. Based on the findings from the static versus dynamic culture conditions, it is feasible to propose that regardless of the scaffold architecture (i.e. bimodal or trimodal), diffusion based in vitro culturing will inevitably lead to non-homogenous cellular distributions which raises important questions regarding scaffold architecture and short-term conditioning of scaffolds in vitro prior to eventual in vivo implantation.

References

1. Chu TM, Halloran JW, Hollister SJ, Feinberg SE. Hydroxyapatite implants with designed internal architecture. J Mater Sci Mater Med. 2001;12:471–8.
2. Woodfield TB, Malda J, de Wijn J, Peters F, Riesle J, van Blitterswijk CA. Design of porous scaffolds for cartilage tissue engineering using a three-dimensional fiber-deposition technique. Biomaterials. 2004;25:4149–61.
3. Hollister SJ. Porous scaffold design for tissue engineering. Nat Mater. 2005;4:518–24.
4. Sachlos E, Czernuszka JT. Making tissue engineering scaffolds work. Review: the application of solid freeform fabrication technology to the production of tissue engineering scaffolds. Eur Cell Mater. 2003;5:29–40.
5. O'Brien FJ, Harley BA, Yannas IV, Gibson L. Influence of freezing rate on pore structure in freeze-dried collagen-GAG scaffolds. Biomaterials. 2004;25:1077–86.
6. Deville S, Saiz E, Tomsia AP. Freeze casting of hydroxyapatite scaffolds for bone tissue engineering. Biomaterials. 2006;27:5480–9.
7. O'Brien FJ, Harley BA, Yannas IV, Gibson LJ. The effect of pore size on cell adhesion in collagen-GAG scaffolds. Biomaterials. 2005;26:433–41.
8. Kim HW, Knowles JC, Kim HE. Hydroxyapatite/poly(epsilon-caprolactone) composite coatings on hydroxyapatite porous bone scaffold for drug delivery. Biomaterials. 2004;25:1279–87.
9. Cyster LA, Grant DM, Howdle SM, Rose FR, Irvine DJ, Freeman D, et al. The influence of dispersant concentration on the pore morphology of hydroxyapatite ceramics for bone tissue engineering. Biomaterials. 2005;26:697–702.
10. Rose FR, Cyster LA, Grant DM, Scotchford CA, Howdle SM, Shakesheff KM. In vitro assessment of cell penetration into porous hydroxyapatite scaffolds with a central aligned channel. Biomaterials. 2004;25:5507–14.
11. Galban CJ, Locke BR. Analysis of cell growth kinetics and substrate diffusion in a polymer scaffold. Biotechnol Bioeng. 1999;65:121–32.
12. Ishaug-Riley SL, Crane-Kruger GM, Yaszemski MJ, Mikos AG. Three-dimensional culture of rat calvarial osteoblasts in porous biodegradable polymers. Biomaterials. 1998;19:1405–12.
13. Leong KF, Cheah CM, Chua CK. Solid freeform fabrication of three-dimensional scaffolds for engineering replacement tissues and organs. Biomaterials. 2003;24:2363–78.
14. Cartmell SH, Porter BD, Garcia AJ, Guldberg RE. Effects of medium perfusion rate on cell-seeded three-dimensional bone constructs in vitro. Tissue Eng. 2003;9:1197–203.
15. Karande TS, Ong JL, Agrawal CM. Diffusion in musculoskeletal tissue engineering scaffolds: design issues related to porosity, permeability, architecture, and nutrient mixing. Ann Biomed Eng. 2004;32:1728–43.
16. Obradovic B, Carrier RL, Vunjak-Novakovic G, Freed LE. Gas exchange is essential for bioreactor cultivation of tissue engineered cartilage. Biotechnol Bioeng. 1999;63:197–205.
17. Obradovic B, Meldon JH, Freed LE, Vunjak-Novakovic G. Glycosaminoglycan deposition in engineered cartilage: experiments and mathematical model. Aiche J. 2000;46:1860–71.
18. Malda J, van den Brink P, Meeuwse P, Grojec M, Martens DE, Tramper J, et al. Effect of oxygen tension on adult articular chondrocytes in microcarrier bioreactor culture. Tissue Eng. 2004;10:987–94.
19. Martin I, Wendt D, Heberer M. The role of bioreactors in tissue engineering. Trends Biotechnol. 2004;22:80–6.
20. Dunn JC, Chan WY, Cristini V, Kim JS, Lowengrub J, Singh S, et al. Analysis of cell growth in three-dimensional scaffolds. Tissue Eng. 2006;12:705–16.
21. Lewis MC, Macarthur BD, Malda J, Pettet G, Please CP. Heterogeneous proliferation within engineered cartilaginous tissue: the role of oxygen tension. Biotechnol Bioeng. 2005;91:607–15.
22. Xu X, Urban JPG, Tirlapur U, Wu MH, Cui Z. Influence of perfusion on metabolism and matrix production by bovine articular chondrocytes in hydrogel scaffolds. Biotechnol Bioeng. 2006;93:1103–11.
23. Freed LE, Langer R, Martin I, Pellis NR, Vunjak-Novakovic G. Tissue engineering of cartilage in space. Proc Natl Acad Sci USA. 1997;94:13885–90.

24. Akmal M, Anand A, Anand B, Wiseman M, Goodship AE, Bentley G. The culture of articular chondrocytes in hydrogel constructs within a bioreactor enhances cell proliferation and matrix synthesis. J Bone Joint Surg Ser B. 2006;88:544–53.

25. Lin AS, Barrows TH, Cartmell SH, Guldberg RE. Microarchitectural and mechanical characterization of oriented porous polymer scaffolds. Biomaterials. 2003;24:481–9.

26. Moore MJ, Friedman JA, Lewellyn EB, Mantila SM, Krych AJ, Ameenuddin S, et al. Multiple-channel scaffolds to promote spinal cord axon regeneration. Biomaterials. 2006;27:419–29.

27. Hadlock T, Sundback C, Hunter D, Cheney M, Vacanti JP. A polymer foam conduit seeded with Schwann cells promotes guided peripheral nerve regeneration. Tissue Eng. 2000;6:119–27.

28. Buckley CT, O'Kelly KU. Development of a hydroxyapatite bone tissue engineering scaffold with a trimodal pore structure. Key Eng Mater. 2008;361–363 II:931–4.

29. Kim YJ, Sah RL, Doong JY, Grodzinsky AJ. Fluorometric assay of DNA in cartilage explants using Hoechst 33258. Anal Biochem. 1988;174:168–76.

30. Wendt D, Jakob M, Martin I. Bioreactor-based engineering of osteochondral grafts: from model systems to tissue manufacturing. J Biosci Bioeng. 2005;100:489–94.

31. Stephan EB, Jiang D, Lynch S, Bush P, Dziak R. Anorganic bovine bone supports osteoblastic cell attachment and proliferation. J Periodontol. 1999;70:364–9.

32. Holy CE, Shoichet MS, Davies JE. Engineering three-dimensional bone tissue in vitro using biodegradable scaffolds: investigating initial cell-seeding density and culture period. J Biomed Mater Res. 2000;51:376–82.

33. Solchaga LA, Tognana E, Penick K, Baskaran H, Goldberg VM, Caplan AI, et al. A rapid seeding technique for the assembly of large cell/scaffold composite constructs. Tissue Eng. 2006;12:1851–63.

34. Wendt D, Marsano A, Jakob M, Heberer M, Martin I. Oscillating perfusion of cell suspensions through three-dimensional scaffolds enhances cell seeding efficiency and uniformity. Biotechnol Bioeng. 2003;84:205–14.

35. Muschler GF, Nakamoto C, Griffith LG. Engineering principles of clinical cell-based tissue engineering. J Bone Joint Surg Am. 2004;86-A:1541–58.